

## On-Chip Manipulation of Single Photons from a Diamond Defect

J. E. Kennard,<sup>1,2</sup> J. P. Hadden,<sup>1</sup> L. Marseglia,<sup>1</sup> I. Aharonovich,<sup>3</sup> S. Castelletto,<sup>4,\*</sup> B. R. Patton,<sup>1</sup> A. Politi,<sup>1,†</sup>  
J. C. F. Matthews,<sup>1</sup> A. G. Sinclair,<sup>2</sup> B. C. Gibson,<sup>4</sup> S. Prawer,<sup>4</sup> J. G. Rarity,<sup>1</sup> and J. L. O'Brien<sup>1</sup>

<sup>1</sup>*H. H. Wills Physics Laboratory & Department of Electrical and Electronic Engineering, Centre for Quantum Photonics, University of Bristol, Merchant Venturers Building, Woodland Road, Bristol BS8 1UB, United Kingdom*

<sup>2</sup>*National Physical Laboratory, Hampton Road, Teddington, Middlesex TW11 0LW, United Kingdom*

<sup>3</sup>*School of Physics and Advanced Materials, University of Technology, Sydney, Post Office Box 123, Broadway, New South Wales 2007, Australia*

<sup>4</sup>*School of Physics, University of Melbourne, Parkville, Victoria 3010, Australia*

(Received 19 April 2013; published 20 November 2013)

Operating reconfigurable quantum circuits with single photon sources is a key goal of photonic quantum information science and technology. We use an integrated waveguide device containing directional couplers and a reconfigurable thermal phase controller to manipulate single photons emitted from a chromium related color center in diamond. Observation of both a wavelike interference pattern and particlelike sub-Poissonian autocorrelation functions demonstrates coherent manipulation of single photons emitted from the chromium related center and verifies wave particle duality.

DOI: [10.1103/PhysRevLett.111.213603](https://doi.org/10.1103/PhysRevLett.111.213603)

PACS numbers: 42.50.Ex, 42.50.Dv, 42.81.Qb, 76.30.Mi

Linear optical circuits (LOCs) are a powerful platform for performing quantum optical experiments [1]. With the addition of high-fidelity photon sources, feed-forward and high-fidelity photon detection, LOCs form a core component of proposed quantum enhanced technologies [2,3] and are a leading platform for performing fundamental quantum experiments [1]. Recently, LOCs have begun to be integrated into monolithic waveguide circuit architectures [4–6]. With inherent interferometric stability and increasing component miniaturization [7], integrated LOCs offer the prospect of performing increasingly complex and flexible quantum optical tasks [6,8], particularly in conjunction with high efficiency on-chip photodetection [9,10]. In previous experiments the photons used in LOCs have been generated by spontaneous parametric sources of photon pairs and subsequent heralding of single photons contaminated by higher photon number terms. Conversely single defect centers in diamond emit via single electron transitions and therefore produce true single photons, even at saturation, making them an attractive scalable photon source for LOCs.

Here we report the coupling of a room temperature color center single photon source and an integrated LOC. The single photons are emitted from a chromium related diamond color center which operates at room temperature [11]. The LOC is a two path interferometer comprised of two directional couplers and an electrically tuned phase shifter on one arm. The LOC enables on-chip manipulation of quantum information encoded onto the path of a verifiable single photon, and contains all of the components required to build arbitrary unitary manipulations. As a demonstration of the combined fidelity of the system, we verify wave-particle duality by utilizing wavelike self interference and particlelike detection statistics observed

simultaneously with this single device. Here we include both directional couplers and active phase shifters (we note that single photons from nitrogen vacancy centers have been coupled to a straight GaP waveguide [12]), which opens up the possibility of using true single photons in complex LOCs, for example studying single photon modal entanglement [13] on a scale of complexity only practically achievable with integrated optics.

SPDC has been a particularly useful source of photons for numerous LOC demonstrations. However, the spontaneous emission statistics of parametric down-conversion means these sources must be operated at low occupation probability to suppress multiphoton terms. Experiments are performed nondeterministically relying on postselection of photons in coincidence. Without the multiplexing of multiple down conversion processes—with heralding detectors, fast switches and optical delay [14,15]—SPDC cannot scale efficiently for many quantum photonics applications. Alternative photon sources, such as quantum dots [16], single atoms [17], ions [18], and dye molecules [19], based on quantized energy transitions, have been employed as single photon sources (SPSs), but require either cryogenic temperatures (dots) or a vacuum environment (atoms, ions) to ensure the requisite identical photons.

Individual diamond defect centers display atomlike optical spectra, with sub-10 nm ZPL linewidths [20], even at room temperature. Thus they are convenient sources of single photons requiring neither trapping nor in principle cryogenic operation, ensuring they are excellent candidates for room temperature sources. Emission linewidths are still orders of magnitude away from being lifetime limited which limits room temperature operation of centers to single photon applications such as quantum key distribution (QKD) [21]. Traditionally, this distinguishability may be overcome

by reducing phonon interactions by placing the color center in a cryogenic environment [22,23]; however, by reducing the available emission density of states through coupling the emitter to a high  $Q$  cavity lifetime limited linewidths could be achieved [24] at or near room temperature.

Here we employ chromium related defect centers, which are particularly bright [25], emitting the majority of photons into the ZPL [11], which facilitates the creation of a high efficiency SPS. The center is created by coimplantation of chromium and oxygen ions using 50 and 19 keV energies, respectively, into type IIa diamond ( $<1$  ppm nitrogen and  $<1$  ppb boron) [26]. The sample is annealed at  $900^\circ\text{C}$  for an hour. Some individual centers do exhibit blinking or photo-bleaching behavior, although this seems to be a symptom of the implantation process, given that chromium related centers in nanodiamond do not [27]. Emission line widths of 4 nm, polarized emission and excited state lifetimes of the order of a nanosecond mean the centers are attractive SPSs for quantum photonic technologies. Because of the inhomogeneous broadening ZPLs are found within the range 730–790 nm ensuring easy integration with existing silica on silicon waveguides, allowing centers to be chosen that emit a wavelength that is inherently low loss. Unlike the negative nitrogen vacancy center (NV), which has two orthogonal dipoles, the chromium related defect's ZPL consists of only a single dipole transition, ensuring all emitted photons have the same linear polarization at room temperature, allowing coherent manipulation within LOCs as waveguide modes are typically polarization dependant. These factors ensure photons emitted from chromium related defects are suitable for observation of single particle quantum behavior in LOCs. Combined with cavity enhanced emission, scalable multiphoton LOC applications would be possible, allowing the replacement of SPDC as the *de facto* single photon source for LOCs.

We report the operation of a diamond color center single photon source in conjunction with a monolithic

LOC waveguide chip. Single photons emitted from a chromium-related color center are guided through the silica-on-silicon circuit [4,28] shown in Fig. 1(a), enabling manipulation of a path encoded qubit and observation of wave and particle effects simultaneously within the single device. The waveguides are lithographically fabricated from silica doped with boron and germanium oxides to control the refractive index, on a silicon substrate. The dopant levels in the core and cladding are controlled to define a refractive index contrast of  $\Delta = 0.5\%$ ; together with a  $3.5\ \mu\text{m} \times 3.5\ \mu\text{m}$  dimension core, the waveguides support only the fundamental mode of near infrared light (in the region of 780 nm light for the purposes of our demonstration, Fig. 1(b) shows the simulated mode for 780 nm light). The waveguide circuit comprises four inputs and four outputs, and four directional couplers,  $DC_{1-4}$ , each with reflectivity  $\eta_i$  and modeled with  $2 \times 2$  transition matrices

$$DC_i = \begin{pmatrix} \sqrt{\eta_i} & i\sqrt{1-\eta_i} \\ i\sqrt{1-\eta_i} & \sqrt{\eta_i} \end{pmatrix}. \quad (1)$$

The circuit is designed to have reflectivities  $\eta_1 = \eta_2 = 1/2$  and  $\eta_3 = \eta_4 = 1/3$ . The basis of the circuit is an interferometer formed from  $DC_1$  and  $DC_2$ , in which the internal phase is controlled via voltage applied across a thermal phase shifter  $\phi$ , fabricated by lithographically patterning a metal layer in the form of a resistive heating element directly above the waveguide and connecting contact pads used to apply voltage (not shown). It is straightforward to compute a  $4 \times 4$  transition matrix that models the circuit ( $U_{\text{chip}}$ ), which shows the single photon entering optical mode  $a$  of the circuit ideally evolves according to

$$a_a^\dagger \xrightarrow{U_{\text{chip}}} \frac{i}{\sqrt{3}} \left( a_e^\dagger - e^{i(\phi/2)} \sin \frac{\phi}{2} a_g^\dagger + e^{i(\phi/2)} \cos \frac{\phi}{2} a_h^\dagger + i e^{i\phi} a_f^\dagger \right). \quad (2)$$

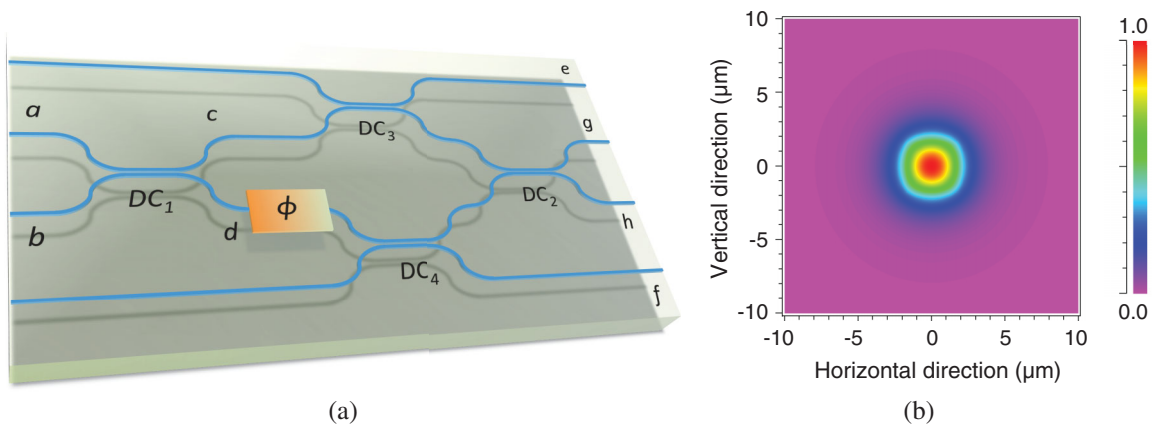


FIG. 1 (color). The silica on silicon waveguide circuit. (a) Silica on silicon waveguide circuit. Directional couplers  $DC_1$  and  $DC_2$  have reflectivity  $= 1/2$  and  $DC_3$  and  $DC_4$  have reflectivity  $= 1/3$ . A resistive heater at waveguide  $d$  allows a relative phase  $\phi$  to be imparted. Photons from an individual chromium related center are coupled into waveguide  $a$  from polarization maintaining fiber (PMF) and are sent to APDs via PMF from waveguides  $e$ – $f$ . (b) Simulated mode of 780 nm light in chip.

Thus, the probability to detect photons at output  $g$  and  $h$  has a sinusoidal phase dependence, enabling wavelike interference fringes to be observed by measuring the rate of photons detected in each arm as a function of phase.

The verification of particlelike behavior is achieved by measuring second order correlation statistics between the output modes. The second order correlation function between two modes is given by  $g^{(2)}(\tau) = \langle I_1(t)I_2(t + \tau) \rangle / \langle I_1(t)I_2(t) \rangle$ . This is obtained experimentally by measuring time intervals between photons detected in each of the two arms after a directional coupler. A single photon entering optical mode  $a$  is detected at each of the output modes with probability given by the modulus square of the amplitudes given in Eq. (2). It takes finite time for a single photon emitter to emit each photon; therefore, the measurement of correlations between the two arms are strongly suppressed for zero time differences. This effect is known as anti-bunching. Since both modes are coupled to the same single photon source, through a directional coupler, this is equivalent to a Hanbury Brown–Twiss style measurement of the second order auto correlation function. Measurement of  $g^{(2)}(0) = 0$  shows that the photons measured are truly emitted in single events.

Centers were addressed optically with a laser scanning fluorescence confocal microscope shown in Fig. 2(a). Off-resonant excitation was achieved via a linearly polarized 27 mW, 690 nm continuous wave diode laser and focused onto the sample with a 0.9 NA microscope objective. The sample was mounted onto a 3-axis piezoelectric stage, allowing both precise location of and stable collection from chromium related centers. Both fluorescence and reflected excitation was collected with the same objective with the fluorescence subsequently transmitted through a 700 nm dichroic mirror. A bandpass filter in the range 770–790 nm enabled rejection of the first and second

order Raman scattering with a half wave plate and linear polarizer aligned vertically for output polarization control. The fluorescence was collected into a single mode 5.0  $\mu\text{m}$  core polarization maintaining fiber, acting as the confocal aperture. Typical count rates when measuring fluorescence from a single chromium related center with silicon APDs were  $0.1 \times 10^6$  counts per sec. Additionally, this light could then be passed to various experiments for analysis. The photon statistics of centers was determined by measuring the second order auto correlation function between two chosen detectors. Figure 2(b) shows the  $g^{(2)}(\tau)$  function for a 778 nm center with its corresponding emission spectrum. The dip at zero delay is characteristic of single photon emission, with  $g^{(2)}(0) = 0.1$ . The deviation from zero is attributed to the convolution of signal with the 500 ps jitter on the detectors, which is comparable to the full width half maximum of the  $g^{(2)}(\tau)$ ,  $\sim 4$  ns.

Single photons from the chromium related centers were fiber butt coupled to the reconfigurable waveguide circuit, detailed above. The outputs of waveguides  $e$ – $h$  were fiber butt coupled and connected to four silicon APDs for measurement. Transmission through the waveguide was typically observed to be  $\sim 60\%$ . To verify the operation of the waveguide circuit, photons from an individual 778 nm center were coupled into waveguide  $a$ . By varying the phase  $\phi$  and measuring the intensity of outputs  $g$  and  $h$ , an interference fringe, as described in Eq. (2), was observed with visibility  $V = (I_{\max} - I_{\min}) / (I_{\max} + I_{\min}) = 0.971 \pm 0.001$ . The full fringe is reproduced in the upper part of Fig. 3(a). Single photon operation was verified by performing a  $g^{(2)}(\tau)$  measurement on the detected signal from modes  $e$  and  $f$ . These equal intensity outputs allowed access to the phase independent part of the modal superposition caused by the  $1/2$  reflectivity directional coupler  $DC_1$ . The lower part of Fig. 3(a) shows a

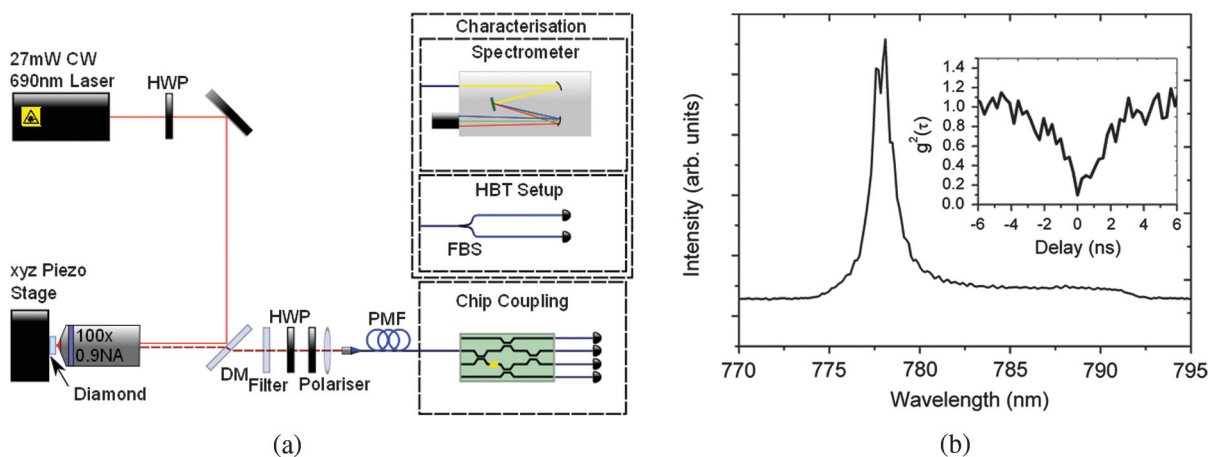


FIG. 2 (color). Experimental setup and characterization of chromium related centers. (a) Schematic diagram of the optical setup used in this Letter. Photons collected from chromium related centers being excited with a 27 mW 690 nm continuous wave laser are fiber coupled and subsequently sent to one of three measurements—a spectrometer, a Hanbury Brown–Twiss correlation setup or the chip described in the main text. (b) The emission spectrum of a chromium related center used in the waveguide experiments. Inset: Second order auto-correlation function of the chromium related center.

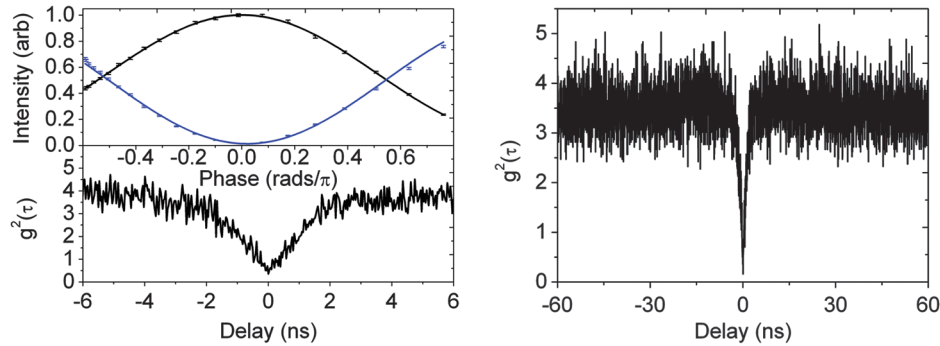


FIG. 3 (color). Experimental data acquired from photons coupled to the integrated waveguide circuit. (a) Above: Intensity measured from waveguides  $g$  and  $h$  as a function of  $\phi$ . The upper (black) line is from waveguide  $h$  and the lower (blue) line is from waveguide  $g$ . Below: Second order auto-correlation function of the chromium related center measured from outputs  $e$  and  $f$ . (b) Second order auto-correlation function of the chromium related center measured from outputs  $h$  and  $f$  when  $\phi = 0$ .

$g^{(2)}(0) = 0.1$ , demonstrating that photons from the chromium related center maintain their particle statistics after transmission through the LOC. The nonzero  $g^{(2)}(0)$  is again explained by the convolution of the signal and detector jitter.

This verifies the expected behavior that single photons within our waveguide circuit show wavelike interference behavior in ports  $g$  and  $h$  and particlelike antibunching behavior in ports  $e$  and  $f$ . However, to demonstrate duality, one would like to demonstrate simultaneous wave and particle effects behavior in the same photons. While performing a second order correlation of the outputs  $g$  and  $h$  and varying  $\phi$  may seem a particularly intuitive method, a  $g^{(2)}(\tau)$  may never be obtained when the system is displaying the strongest wavelike behavior—full constructive or destructive interference, when  $\phi = n\pi$ . To investigate duality at this point, a  $g^{(2)}(\tau)$  was measured from modes  $h$  and  $f$  when  $\phi = 0$ . At this point, since destructive interference suppresses photon detection in mode  $g$ , any photons detected at  $h$  must have previously displayed wavelike behavior. Figure 3(b) shows that the operation displays clear antibunching, with  $g^{(2)}(0) = 0.1$ , indicating that the photons detected in  $h$  must have demonstrated wavelike properties in the interferometer, while subsequently being demonstrated to be individual photons by the Hanbury Brown–Twiss experiment. Consequently, the photons must have displayed a wavelike phenomenon within the interferometer and particlelike after  $DC_2$ , thereby verifying the principles of both complementarity and duality. Previous experiments have demonstrated wave-particle duality by switching apparatus between an interferometer and a Hanbury Brown–Twiss setup, or placing them in series and observing an interference fringe and an averaged  $g^{(2)}(\tau)$  simultaneously [29–31]. Additional verification has been displayed by the implementation of a delayed choice experiment [32]. Our experiment not only extends these previous experiments by ensuring that wave particle duality is verified with maximum wave interference visible, but acts as an evaluation of the combination of the two systems.

We have operated an integrated LOC circuit with single photons from a chromium-related diamond defect center. Despite some individual centers lacking photostability, the high emission rates, linearly polarized emission, and low degree of phonon coupling of the chromium related defect make it an excellent candidate SPS for LOCs. ZPL emission in the near infrared that matches the high transmission and detection efficiencies of current waveguides and detectors technologies is also a key advantage. The high fidelity control of single photons reported here demonstrates the feasibility of manipulating single photon states emitted from other diamond color centers, and the possibility to harness more complex LOCs. Furthermore, collection of photons could be improved with on-diamond structures such as SILs [33,34] or by integrating chromium related centers and waveguides onto a single monolithic device, a possibility with chromium related centers in nanodiamond [27], which would both enhance the coupling efficiency and reduce experimental complexity, allowing many chromium related centers to be used in a single device. As with other diamond defect centers, at room temperature the emission linewidth of the chromium related center is not lifetime limited, causing the indistinguishability of sequentially emitted photons to be exceedingly low. While our experiment makes no attempt to modify the emission properties of the center to this effect, the prospect of cavity enhanced emission could enable the chromium related center to produce highly indistinguishable photons [24], making it a strong candidate SPS for LOCs for fundamental physics and quantum technologies, particularly when combined with integrated LOCs as demonstrated here.

The authors are grateful for financial support from DIAMANT, EPSRC, and ERC. This work was carried out with the support of the Bristol Centre for Nanoscience and Quantum Information. J.E.K. is supported by a EPSRC Industrial CASE studentship from NPL. J.L.OB. acknowledges a Royal Society Wolfson Merit Award and a Royal Academy of Engineering Chair

in Emerging Technologies. J.C.F.M. is supported by a Leverhulme Trust Early Career Fellowship. The authors would like to acknowledge Brett Johnson and Jeff McCallum for useful advice and discussion. The Department of Electronic Materials Engineering at the Australian National University is acknowledged for the access to the implantation facilities. I. A. is the recipient of an Australian Research Council Discovery Early Career Research ward (Project No. DE130100592).

\*Present address: School of Aerospace, Mechanical and Manufacturing Engineering, RMIT University, Melbourne, Australia.

†Present address: School of Physics and Astronomy, University of Southampton, Southampton SO17 1BJ, United Kingdom.

- [1] J.-W. Pan, Z.-B. Chen, C.-Y. Lu, H. Weinfurter, A. Zeilinger, and M. Żukowski, *Rev. Mod. Phys.* **84**, 777 (2012).
- [2] E. Knill, R. Laflamme, and G.J. Milburn, *Nature (London)* **409**, 46 (2001).
- [3] J.L. O'Brien, A. Furusawa, and J. Vuckovic, *Nat. Photonics* **3**, 687 (2009).
- [4] A. Politi, M.J. Cryan, J.G. Rarity, S. Yu, and J.L. O'Brien, *Science* **320**, 646 (2008).
- [5] A. Peruzzo, P. Shadbolt, N. Brunner, S. Popescu, and J.L. O'Brien, *Science* **338**, 634 (2012).
- [6] P.J. Shadbolt, M.R. Verde, A. Peruzzo, A. Politi, A. Laing, M. Lobino, J.C.F. Matthews, M.G. Thompson, and J.L. O'Brien, *Nat. Photonics* **6**, 45 (2011).
- [7] D. Bonneau *et al.*, *New J. Phys.* **14**, 045003 (2012).
- [8] A. Peruzzo *et al.*, *Science* **329**, 1500 (2010).
- [9] J.P. Sprengers *et al.*, *Appl. Phys. Lett.* **99**, 181110 (2011).
- [10] W.H.P. Pernice, C. Schuck, O. Minaeva, M. Li, G.N. Goltsman, A.V. Sergienko, and H.X. Tang, *Nat. Commun.* **3**, 1325 (2012).
- [11] I. Aharonovich, S. Castelletto, D.A. Simpson, A.D. Greentree, and S. Prawer, *Phys. Rev. A* **81**, 043813 (2010).
- [12] K.-M.C. Fu, C. Santori, P.E. Barclay, I. Aharonovich, S. Prawer, N. Meyer, a.M. Holm, and R.G. Beausoleil, *Appl. Phys. Lett.* **93**, 234107 (2008).
- [13] S.B. Papp, K.S. Choi, H. Deng, P. Lougovski, S.J. van Enk, and H.J. Kimble, *Science* **324**, 764 (2009).
- [14] A.L. Migdall, D. Branning, and S. Castelletto, *Phys. Rev. A* **66**, 053805 (2002).
- [15] X.-S. Ma, S. Zotter, J. Kofler, T. Jennewein, and A. Zeilinger, *Phys. Rev. A* **83**, 043814 (2011).
- [16] S. Kako, C. Santori, K. Hoshino, S. Göttinger, Y. Yamamoto, and Y. Arakawa, *Nat. Mater.* **5**, 887 (2006).
- [17] A. Kuhn, M. Hennrich, and G. Rempe, *Phys. Rev. Lett.* **89**, 067901 (2002).
- [18] M. Keller, B. Lange, K. Hayasaka, W. Lange, and H. Walther, *Nature (London)* **431**, 1075 (2004).
- [19] J. Hwang and E.A. Hinds, *New J. Phys.* **13**, 085009 (2011).
- [20] I. Aharonovich, S. Castelletto, D.A. Simpson, C.-H. Su, A.D. Greentree, and S. Prawer, *Rep. Prog. Phys.* **74**, 076501 (2011).
- [21] A. Beveratos, R. Brouri, T. Gacoin, A. Villing, J.-P. Poizat, and P. Grangier, *Phys. Rev. Lett.* **89**, 187901 (2002).
- [22] H. Bernien, L. Childress, L. Robledo, M. Markham, D. Twitchen, and R. Hanson, *Phys. Rev. Lett.* **108**, 043604 (2012).
- [23] A. Sipahigil, M.L. Goldman, E. Togan, Y. Chu, M. Markham, D.J. Twitchen, A.S. Zibrov, A. Kubanek, and M.D. Lukin, *Phys. Rev. Lett.* **108**, 143601 (2012).
- [24] H. Kaupp, C. Deutsch, and H. Chang, [arXiv:1304.0948v1](https://arxiv.org/abs/1304.0948v1).
- [25] I. Aharonovich, S. Castelletto, B.C. Johnson, J.C. McCallum, D.A. Simpson, A.D. Greentree, and S. Prawer, *Phys. Rev. B* **81**, 121201 (2010).
- [26] I. Aharonovich, S. Castelletto, B.C. Johnson, J.C. McCallum, and S. Prawer, *New J. Phys.* **13**, 045015 (2011).
- [27] I. Aharonovich, S. Castelletto, D.A. Simpson, A. Stacey, J. McCallum, A.D. Greentree, and S. Prawer, *Nano Lett.* **9**, 3191 (2009).
- [28] J.C.F. Matthews, A. Politi, D. Bonneau, and J.L. O'Brien, *Phys. Rev. Lett.* **107**, 163602 (2011).
- [29] P. Grangier, G. Roger, and A. Aspect, *Europhys. Lett.* **1**, 173 (1986).
- [30] C. Braig, P. Zarda, C. Kurtsiefer, and H. Weinfurter, *Appl. Phys. B* **76**, 113 (2003).
- [31] T. Aichele, *AIP Conf. Proc.* **750**, 35 (2005).
- [32] V. Jacques, E. Wu, F. Grosshans, F. Treussart, P. Grangier, A. Aspect, and J.-F. Roch, *Phys. Rev. Lett.* **100**, 220402 (2008).
- [33] J.P. Hadden, J.P. Harrison, A.C. Stanley-Clarke, L. Marseglia, Y.-L.D. Ho, B.R. Patton, J.L. O'Brien, and J.G. Rarity, *Appl. Phys. Lett.* **97**, 241901 (2010).
- [34] L. Marseglia *et al.*, *Appl. Phys. Lett.* **98**, 133107 (2011).